

Residue-specific immobilization of protein molecules by size-selected clusters

Umberto Prisco, Carl Leung, Chrisa Xirouchaki, Celine H Jones, John K Heath and Richard E Palmer

J. R. Soc. Interface 2005 **2**, 169-175

doi: 10.1098/rsif.2005.0032

References

This article cites 27 articles, 2 of which can be accessed free

<http://rsif.royalsocietypublishing.org/content/2/3/169.full.html#ref-list-1>

Email alerting service

Receive free email alerts when new articles cite this article - sign up in the box at the top right-hand corner of the article or click [here](#)

To subscribe to *J. R. Soc. Interface* go to: <http://rsif.royalsocietypublishing.org/subscriptions>

Residue-specific immobilization of protein molecules by size-selected clusters

Umberto Prisco¹, Carl Leung¹, Chrisa Xirouchaki¹, Celine H. Jones²,
John K. Heath² and Richard E. Palmer^{1,†}

¹ Nanoscale Physics Research Laboratory, School of Physics and Astronomy, and

² School of Biosciences, The University of Birmingham, Edgbaston,
Birmingham B15 2TT, UK

The atomic force microscope (AFM), operating in contact mode, has been employed in buffer solution to study two proteins; (i) green fluorescent protein (GFP), from the hydromedusan jellyfish *Aequorea victoria*; and (ii) human oncostatin M (OSM), in the presence of size-selected gold nanoclusters pinned on to a highly oriented pyrolytic graphite substrate. The AFM images have revealed immobilization of single molecules of OSM, which are strongly bound to the gold nanoclusters. Conversely, no strong immobilization has been observed for the GFP, as these molecules were easily displaced by the scanning tip. The contrasting behaviour of the two proteins can be explained by the exposed molecular surface area of their cysteine residues as modelled on the basis of their respective X-ray crystallographic data structures. GFP contains two cysteine residues, but neither is readily available to chemisorb on the gold clusters, because the cysteines are largely inaccessible from the surface of the protein. In contrast, OSM has a total of five cysteine residues, with different degrees of accessibility, which make the protein amenable to anchoring on the nanoclusters. Statistical analysis of the height of the OSM molecules bound to the nanoclusters is in accordance with crystallographic data, and suggests various configurations of the proteins on the clusters, associated with the presence of different cysteine anchoring sites. These results suggest that the three-dimensional conformation of protein molecules is preserved when they are chemisorbed to size-selected gold clusters, thus opening a new route towards oriented immobilization of individual protein molecules.

Keywords: atomic force microscopy; single molecule; cysteine; molecular surface area; gold clusters; oriented immobilization

1. INTRODUCTION

The stable immobilization of individual protein molecules, with controlled orientation (such that their active site(s) are accessible), is a growing challenge, for example, in the development and application of bioelectronic devices (Willner & Willner 2001). Much effort has been dedicated to the atomic force microscope (AFM) or scanning tunnelling microscopy (STM) characterization of proteins chemisorbed on to extended gold surfaces (Friis *et al.* 1997a; Schnyder *et al.* 2002; Bizzarri *et al.* 2003a). One approach is to engineer a mutant version of the protein by introducing a cysteine residue or disulphide bond to allow for stable immobilization on gold supports (Friis *et al.* 1997b; Kanno *et al.* 2000; Andolfi *et al.* 2002; Bizzarri *et al.* 2003a). These experimental studies have been supported by molecular dynamics simulations of the interaction between proteins and an extended gold substrate (Bizzarri *et al.* 2003a,b). Thus far, the gold

substrates have consisted of evaporated films or large islands, which do not allow the immobilization of isolated proteins, often resulting in the creation of protein monolayers on the surface. A monolayer is less attractive compared with individual protein attachment for specific site recognition studies, as large areas within the protein are sacrificed owing to neighbouring protein–protein interactions. An elegant approach to this problem is to immobilize proteins on to a surface (e.g. a highly oriented pyrolytic graphite substrate (HOPG)) decorated with size-selected gold (Au) clusters deposited from a cluster-beam source. This has been demonstrated for the chaperone protein GroEL and the enzyme horseradish peroxidase, apparently chemisorbed, via free cysteine residues and disulphide bridges, respectively (Palmer *et al.* 2003; Leung *et al.* 2004). Here, we report a comparative study of two functionally important model proteins, green fluorescent protein (GFP) and human oncostatin M (OSM), exploring the nature of the interaction between the protein molecules and gold clusters (pinned on HOPG), and its consequences for the molecular orientation.

†Author for correspondence (r.e.palmer@bham.ac.uk).

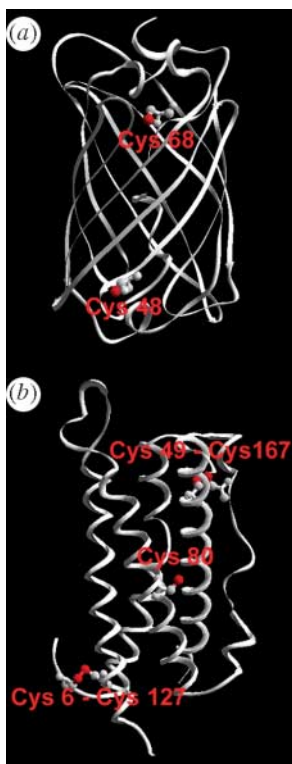


Figure 1. (a) The ‘ β -can’ structure of GFP, the molecule is about $45 \times 35 \times 35 \text{ \AA}$ in size. (b) Structure of OSM, the molecule is about $60 \times 24 \times 20 \text{ \AA}$. The cysteine residues are represented by balls and sticks, and the sulphur atoms are coloured red. Crystallographic data adapted from the Protein Data Bank (<http://www.rcsb.org/pdb>).

GFP is a 26 kDa fluorescent protein consisting of 236 amino acids isolated from *Aequorea victoria*. The fluorescence spectrum peaks at 509 nm with a shoulder at 540 nm. This offers considerable scope as a non-invasive marker in cells, and is used in many applications, such as cell lineage tracing and gene expression reporting (Zimmer 2002; Lippincott-Schwartz *et al.* 2003; Baruch *et al.* 2004). Structurally, a single GFP molecule has a cylindrical shape, consisting of 11 strands of β -sheet on the outside, with an α -helix on the inside forming a ‘ β -can’, as illustrated in figure 1a (Ormo *et al.* 1996). It has two cysteine residues along the backbone: Cys 48 and Cys 68.

OSM is a 21 kDa growth-regulating protein comprising 187 amino acids and belonging to the cytokine family. It exerts inhibitory effects on the growth of A375 melanoma, lung carcinomas and other cancers (Kishimoto *et al.* 1994; Robinson *et al.* 1994; Economides *et al.* 1995). A molecule of OSM contains five cysteine residues, as shown in figure 1b. Four of these residues form disulphide bonds (Cys 6–Cys 127 and Cys 49–Cys 167), leaving one lone cysteine residue, Cys 80 (Deller *et al.* 2000).

These two proteins are structurally and kinetically well-characterized proteins, but present quite different arrangements of cysteine residues in their tertiary structures. The AFM images reveal that single OSM molecules are chemisorbed on to the gold nanoclusters, while there is no strong interaction between the GFP and the clusters. Indeed, the GFP molecules are only

weakly adsorbed on the surface, such that they are wiped by the scanning tip. The topology of the immobilized OSM molecules was statistically analysed. The height distribution is in agreement with the crystallographic data in the hypothesis of a non-denaturing immobilization on gold clusters through accessible cysteine residues. Local peaks in the height distribution are assigned to the different orientations of the OSM molecules on the nanoclusters arising from the various cysteine anchoring points accessible on the protein surface.

2. EXPERIMENTAL

Purification of GFP and OSM was performed following well-established methods. The protein solution concentration is an important factor to obtain good results. Hitherto, relatively large concentrations (greater than $1 \mu\text{g ml}^{-1}$) of proteins were used, which densely covered the graphite substrate; this generally results in large protein islands or complexes, which are relatively easy to image (Palmer *et al.* 2003; Collins *et al.* 2004; Leung *et al.* 2004). The solutions used in our experiments were serially diluted to a final concentration of about one protein per nanocluster, with the aim of providing a large population of single protein molecules bound to single clusters.

The cluster samples were produced by the cluster-pinning method reported by Carroll *et al.* (2000) (see also Helmer 2000). Size-selected metal (Au) clusters were generated by a magnetron sputtering, gas condensation cluster-beam source, and mass selected to within 5% by a novel, lateral time-of-flight mass filter, as previously described (von Issendorff & Palmer 1999; Pratontep *et al.* 2003). The energetic beam of ionized gold clusters was deposited on an HOPG substrate with sufficient kinetic energy to ‘pin’ the clusters at their individual points of impact on the graphite surface (between 12 and 18 eV atom^{-1}). The size-selected clusters for the experiments consisted of 26, 40, 55 or 70 atoms, and the mean distance between deposited clusters on the surface (typically about 20 nm), is controlled by the cluster-beam deposition time. The clusters usually adopt a two-dimensional platelet morphology owing to the energetic impact on the surface, and range between 2 and 4 nm in size.

The HOPG substrates employed were rectangular (about $10 \times 5 \text{ mm}$), with the size-selected clusters decorating an inner, circular region of about 3 mm in diameter. Forty microlitres of the diluted protein solution was pipetted on to the HOPG sample and left to incubate for 3 h at room temperature, to allow the proteins to probe the size-selected clusters. The sample was enclosed by a glass beaker to minimize evaporation of the protein solution. After incubation, the sample was gently rinsed with ultrapure water (resistivity greater than $18 \text{ M}\Omega \text{ cm}^{-1}$) to remove weakly adsorbed proteins, and thereafter covered with buffer solution for AFM imaging. Two different imaging buffers were used in these experiments: 172 mM PBS and 55 mM MES. An additional drop of the buffer solution used for imaging (approximately

30 μ l) was carefully placed on the tip, which was carefully lowered so that the two drops joined up, forming a continuous liquid layer between the AFM cantilever and the sample surface. A further half an hour was needed to attain thermal equilibrium before imaging. Periodically, more ultrapure water was added to maintain the liquid layer on the substrate.

The AFM imaging was carried out with a Digital Instruments dimension 3100, equipped with a 90 μ m scan head, in contact mode. A liquid cell was used with a skirt seal to prevent ingress of liquid. During scanning, the force between the tip and the surface was kept constant to about 0.5 nN to avoid any damage to the proteins. Commercial oxide-sharpened silicon nitride cantilevers (Olympus) with a nominal tip radius of 20 nm and a spring constant of 0.09 N m⁻¹ were used. As a control, HOPG substrates with size-selected clusters were imaged in the same conditions, but without the addition of protein. All experiments were performed at room temperature, and the images with 512 \times 512 pixels were collected without further image processing.

3. AFM RESULTS

Many attempts were made to immobilize the GFP protein on to different size-selected clusters on HOPG, namely Au₂₆, Au₅₅ and Au₇₀, under a variety of buffers and pH values. However, the resulting AFM images clearly indicate that GFP does not bind to the gold nanoclusters. At sub monolayer concentrations of the protein, neither stable single proteins nor protein agglomerates could be repeatedly imaged in the central cluster area. The behaviour of the protein is the same outside the cluster region, i.e. on the bare graphite surface. After the first scan, even with minimum contact force, the proteins were displaced by the action of the tip, and at times aggregated at the HOPG steps. This situation is typical of other proteins on bare HOPG (Sarno *et al.* 2003). A typical result of a scan in the cluster area of a graphite surface decorated with Au₇₀ nanoclusters is shown in figure 2. The protein concentration used in this experiment was 0.22 μ g ml⁻¹ (8.2 nM), and the imaging buffer was 55 mM 2-(4-morpholino)-ethane sulphonate (MES) at pH 6.4. The imaging parameters were chosen to increase the possibility of observing the proteins if they were bound to the nanoclusters. Indeed, at a pH of 6.4, both the GFP (isoelectric point at pH 5 (Richards *et al.* 1999)) and the Si₃N₄ tip (isoelectric point at pH 6) are negatively charged. In these conditions, the interaction force between the AFM tip and the protein is strongly repulsive owing to the low electrolyte concentration (Israelachvili 1992; Rossell *et al.* 2003), and the tip is likely to provide an overestimate of the protein height, thereby increasing its 'sensitivity'. Figure 2a shows an area within the cluster region of the sample where 'wavy lines' are formed, but the GFP is not immobilized, as these features are clearly moved across the surface (as shown in figure 2b) and collected from the same area after about five consecutive scans. Figure 2c was obtained by zooming

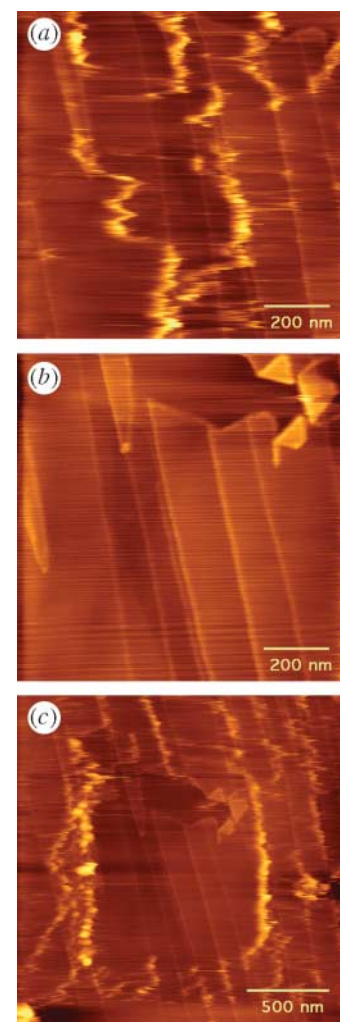


Figure 2. (a) AFM image in buffer solution of a gold nanocluster area on graphite after GFP deposition. (b) The same area as in (a), after five scans. Zooming out from (b) yields (c), showing the area swept clear by the tip and protein aggregation at the edges.

out from the previous area. The square region that has been wiped clear of proteins is visible and demonstrates that GFP is not immobilized by the size-selected nanoclusters.

On the other hand, OSM is readily immobilized on to the size-selected gold nanoclusters. The results of an immobilization with Au₄₀ clusters on graphite are shown in figure 3a,b. The protein concentration used in this experiment was 0.15 μ g ml⁻¹ (5.7 nM) and the imaging buffer was 172 mM phosphate buffer saline (PBS) at a pH of 7.3. Figure 3a shows a 1.7 \times 1.7 μ m scan of the surface within the cluster-decorated area. As compared with figure 2, stable globular features are visible on the surface, which are attributed to the protein molecules immobilized on to the clusters. The graphite steps are also clearly recognizable in figure 3a. The observed protein features were stable after repeated scans, and also with an increased value of the interaction force between tip and surface. When the applied force was increased, the imaged protein features were seen to be stretched laterally by the tip, but immediately after reducing the applied force to 0.5 nN,

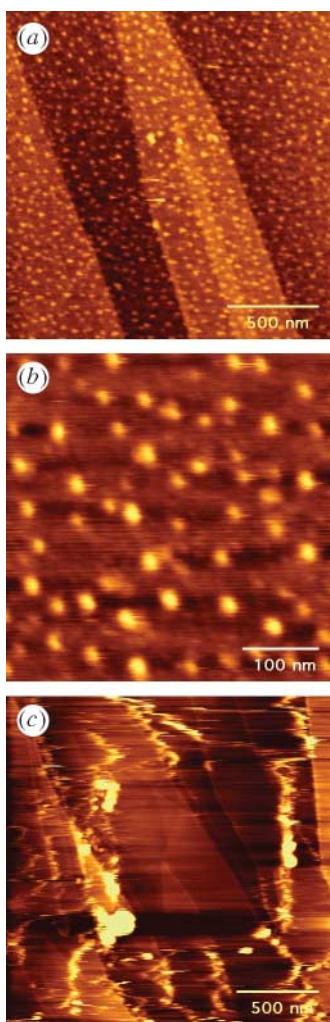


Figure 3. (a) AFM image in buffer solution of the gold nanocluster area on graphite after OSM deposition. The surface is decorated with globular features that are stable under repeated scanning by the AFM tip. (b) Smaller area from (a), revealing individual OSM molecules on Au_{40} clusters. (c) AFM image of OSM outside the nanocluster area displaying the weak interaction of the OSM with the bare graphite substrate (cf. figure 2c).

they regained their original globular shape. Figure 3b is a magnified image of the OSM molecules on the size-selected Au_{40} nanoclusters. The immobilized proteins were stable when imaged again after several days. Moreover, the experiment was repeated with Au_{55} clusters with similar results. No immobilized proteins were observed outside the cluster area, as illustrated in figure 3c.

4. DISCUSSION

The location of the cysteine residues within the protein structure is crucial in accounting for the contrasting behaviour of the GFP and OSM molecules in the presence of gold nanoclusters. In the simplest case, a cysteine residue buried inside a protein is not accessible to the solvent, and by extension is inaccessible to the size-selected cluster, barring any conformational changes in the protein structure. Likewise, the degree of accessibility of a

Table 1. Molecular surface area (MSA) results for the Cys residues in GFP and OSM, and also of the corresponding sulphur atoms.

(Values quoted are in \AA^2 and calculations were performed in SURFRACE (Tsodikov *et al.* 2002) using a 1.4 \AA probe radius).

	residue	MSA (residue)	MSA (sulphur)
green fluorescent protein	Cys 48	10.26	0
	Cys 68	0	0
oncostatin M	Cys 6	48.2	15.26
	Cys 49	13.45	0
	Cys 80	59.42	32.97
	Cys 127	14.36	14.36
	Cys 167	0	0

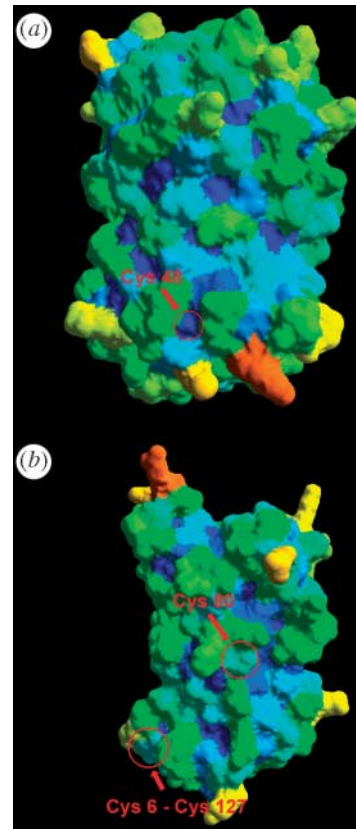


Figure 4. (a) The molecular surface of GFP with colour-coded accessibilities, yellow regions are the most accessible, while dark blue regions are the least accessible. Only a small portion of the Cys 48 is visible compared with (b), the molecular surface of OSM where Cys 80 and the disulphide bridge Cys 6–Cys 147 both present large accessible areas for chemisorption on to gold nanoclusters.

cysteine residue near the protein surface can also vary. To gain better insight into the levels of accessibility of the cysteine residues and the sulphur atoms therein (which can bond to the gold clusters), we have adopted the notion of molecular surface area. This is defined as the contact surface area of a solvent probe sphere that rolls along the surface of the protein (Richards 1977), as obtained in practice from the software package SURFRACE (Tsodikov *et al.*

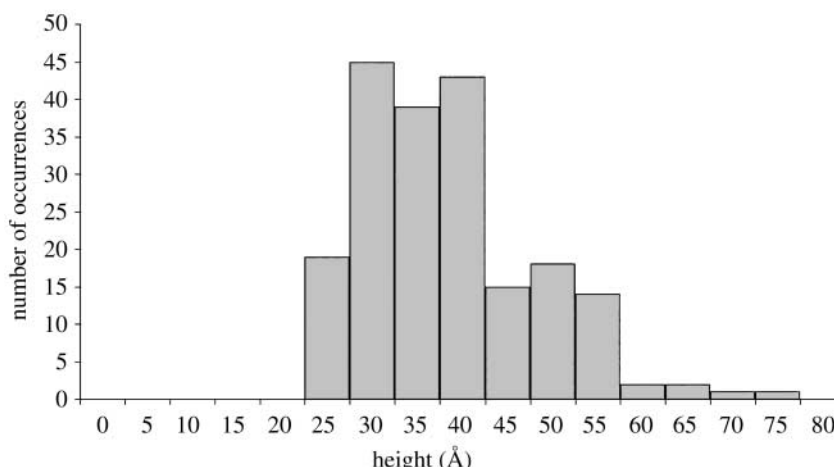


Figure 5. Histogram of the maximum height distribution of 200 OSM molecules immobilized on Au_{40} nanoclusters on graphite.

2002). It can be logically assumed that the larger the exposed molecular surface area associated with a particular residue (or even sulphur atom), the more accessible it is to an external probe, such as the gold nanoclusters in our experiments. The results of these calculations, performed on both the GFP and the OSM molecules are summarized in table 1. A probe radius of 1.4 \AA is used in these calculations as it corresponds to the radius of a water molecule (Richards 1977; Tsodikov *et al.* 2002). Incidentally, this value is also very close to the atomic radius of the gold atom ($1.4\text{--}1.7\text{ \AA}$), which suggests that a gold atom within a cluster is effectively acting as a probe on the protein surface.

The molecular surface-area calculations reveal that the entirety of Cys 68 in the GFP is well buried within the can-like structure of the protein, and therefore it is inaccessible to the probe. The Cys 48 residue in the GFP is marginally exposed, with an area of about 10 \AA^2 . However, this contribution is due to the backbone of the amino acid, and not the sulphur atom. Furthermore, since Cys 48 lies within a rigid beta sheet, and the sulphur atom is directed towards the inside of the GFP molecule as illustrated in figure 1, it is even less likely to be available for binding to the nanoclusters. When the molecular surface of the GFP is visualized as in figure 4a, the backbone of the Cys 48 is almost visible, but not the sulphur atom. The observed behaviour of the GFP is thus evidence that the protein retains its native conformation in the presence of the size-selected gold nanoclusters.

The five cysteine residues of the OSM molecule present a range of molecular surface areas. Cys 49 in the OSM is a similar case to Cys 48 in the GFP, in that its contribution towards the molecular surface area is from the amino acid backbone, but not from the sulphur atom. Cys 49 is covalently linked to Cys 167, which is effectively buried, and hence the resulting disulphide bridge is unavailable for binding to the gold nanoclusters. However, the combination of Cys 6 and Cys 127 forms another disulphide bridge in which both sulphur atoms contribute equally

(approximately 15 \AA^2 each) to the molecular surface areas of their respective residues. Moreover, it should be noted that the sulphur in Cys 127 is the only portion of the residue that is on the molecular surface. It can be envisaged that this particular disulphide bridge could act as a potential binding site to the gold nanoclusters. The lone Cys 80 has the most accessible surface (in table 1), with the sulphur contributing (approximately 33 \AA^2) more than half of the molecular surface area of the residue. Figure 4b illustrates the molecular surface of OSM and it is clear that the Cys 80 and the disulphide bridge Cys 6 and Cys 127 are the most likely candidate residues to bind to the gold nanoclusters. Cys 49 and Cys 167, which are crucial to the biological activity of the protein, are not anticipated to interact with the gold clusters as discussed. As a result, different orientations of the immobilized OSM proteins might be expected on the surface and thus manifested in the AFM height data. A variety of protein arrangements on gold films has already been theoretically modelled for other proteins (Bizzarri *et al.* 2003a). In the case of Cys 80–Au binding for OSM, the height should be about 20 \AA , with the molecule lying flat on the surface. If the disulphide bridge Cys 6–Cys 127 is the binding site, the height can take a spread of values between 24 and 45 \AA (based on crystallographic data), as the OSM may hinge about the disulphide bridge while being scanned by the AFM tip. Statistical analysis of the height of the OSM array on the size-selected Au nanoclusters on graphite is shown in figure 5. The height plot can be interpreted as a bimodal distribution; a first strong maximum at $30\text{--}40\text{ \AA}$ and a second weaker maximum at 50 \AA , suggestive of the two predicted orientations of the protein on the surface. We note that deformation of a protein is possible even at the minimal applied force (Muller *et al.* 1999).

5. CONCLUSION

Two proteins, GFP and OSM, with different accessibilities to their cysteine residues, have been imaged in the presence of size-selected gold nanoclusters pinned

on to graphite substrates. *In situ* AFM imaging of the proteins on these substrates has determined that GFP does not immobilize on the gold nanoclusters, whereas OSM forms stable, dispersed protein arrays on the surface. These experiments were carried out with size-selected clusters of 26, 40, 55 and 70 atoms. It is clear that the presence of cysteine residues in a protein does not guarantee that the latter will covalently bind to a size-selected gold nanocluster (or an extended gold surface). The contrasting behaviour of the two proteins has been investigated by applying the concept of molecular surface area to the proteins to characterize the accessibility of the individual cysteine residues, and most crucially, the sulphur atoms therein, which can form a covalent bond with the gold nanoclusters. In OSM, the sulphur atoms in the Cys 80 and Cys 6–Cys 127 bridge, all lie on the molecular surface of the protein, unlike any of the sulphur atoms in GFP. The fact that GFP is not immobilized by the gold nanoclusters also implies that GFP retains its native structure while it is probing the gold nanoclusters on the graphite surface, since the cysteines buried in the protein might be released for binding if the protein denatured locally or completely. When the proteins are immobilized by the gold nanoclusters, as exemplified by OSM, specific orientation(s) of the molecule can be conferred, as consistent with the AFM height distributions. The creation of tailored binding sites for protein chemisorption, based on cluster deposition on inert surfaces, thus appears to represent an attractive route towards single molecule science studies of protein morphology and interactions.

U.P. acknowledges AFM training from Dr John Collins, University of Birmingham and valuable discussions with Professor Xinyong Chen, University of Nottingham. We thank the EU Research Training Network ‘Micro-Nano’, Cancer Research UK, the EPSRC and the University of Birmingham for financial support of this work.

REFERENCES

Andolfi, L., Cannistraro, S., Canters, G. W., Facci, P., Ficca, A. G., van Amsterdam, M. A. & Verbeet, M. Ph. 2002 A poplar plastocyanin mutant suitable for adsorption onto gold surface via disulfide bridge. *Arch. Biochem. Biophys.* **399**, 81.

Baruch, A., Jeffery, D. A. & Bogyo, M. 2004 Enzyme activity—it’s all about image. *Trends Cell Biol.* **14**, 29.

Bizzarri, A. R., Bonanni, B., Costantini, G. & Cannistraro, S. 2003 A combined atomic force microscopy and molecular dynamics simulation study on a plastocyanin mutant chemisorbed on a gold surface. *Chemphyschem.* **4**, 1189.

Bizzarri, A. R., Costantini, G. & Cannistraro, S. 2003 MD simulation of a plastocyanin mutant adsorbed onto a gold surface. *Biophys. Chem.* **106**, 111.

Carroll, S. J., Pratontep, S., Streun, M., Palmer, R. E., Hobday, S. & Smith, R. 2000 Pinning of size-selected Ag clusters on graphite surfaces. *J. Chem. Phys.* **113**, 7723.

Collins, J. C., Xirouchaki, C., Palmer, R. E., Heath, J. K. & Jones, C. H. 2004 Clusters for biology: immobilization of proteins by size-selected metal clusters. *Appl. Surf. Sci.* **226**, 197.

Deller, M. C., Hudson, K. R., Ikemizu, S., Bravo, J., Jones, E. Y. & Heath, J. K. 2000 Crystal structure and functional dissection of the cytostatic cytokine oncostatin M. *Structure* **8**, 863.

Economides, A. N., Ravetch, J. V., Yancopoulos, G. D. & Stahl, N. 1995 Designer cytokines—targeting actions to cells of choice. *Science* **270**, 1351.

Friis, E. P., Andersen, J. E. T., Madsen, L. L., Møller, P. & Ulstrup, J. 1997a *In situ* STM and AFM of the copper protein *Pseudomonas aeruginosa* azurin. *J. Electroanal. Chem.* **431**, 35.

Friis, E. P., Andersen, J. E. T., Madsen, L. L., Bonander, N., Møller, P. & Ulstrup, J. 1997b Dynamics of *Pseudomonas aeruginosa* azurin and its Cys3Ser mutant at single-crystal gold surfaces investigated by cyclic voltammetry and atomic force microscopy. *Electrochim. Acta* **42**, 2889.

Helmer, M. 2000 Nanotechnology: pinning on impact. *Nature—News and Views* **408**, 531.

Israelachvili, J. 1992 *Intermolecular and surface forces*. London: Academic Press.

Kanno, S., Yanagida, Y., Haruyama, T., Kobatake, E. & Aizawa, M. 2000 Assembling of engineered IgG-binding protein on gold surface for highly oriented antibody immobilization. *J. Biotechnol.* **76**, 207.

Kishimoto, T., Taga, T. & Akira, S. 1994 Cytokine signal-transduction. *Cell* **76**, 253.

Leung, C., Xirouchaki, C., Berovic, N. & Palmer, R. E. 2004 Immobilization of protein molecules by size-selected metal clusters on surfaces. *Adv. Mater.* **16**, 223.

Lippincott-Schwartz, J., Altan-Bonnet, N. & Patterson, G. H. 2003 Photobleaching and photoactivation: following protein dynamics in living cells. *Nat. Cell Biol.*, S7–S14.

Muller, D. J., Fotiadis, D., Scheuring, S., Muller, S. A. & Engel, A. 1999 Electrostatically balanced subnanometer imaging of biological specimens by atomic force microscope. *Biophys. J.* **76**, 1101.

Ormo, M., Cubitt, A. B., Kallio, K., Gross, L. A., Tsien, R. Y. & Remington, S. J. 1996 Crystal structure of the *Aequorea victoria* green fluorescent protein. *Science* **273**, 1392.

Palmer, R. E., Pratontep, S. & Boyen, H. G. 2003 Nanostructured surfaces from size-selected clusters. *Nat. Mater.* **2**, 443.

Pratontep, S., Preece, P., Xirouchaki, C., Palmer, R. E., Sanz-Navarro, C. F., Kenny, S. D. & Smith, R. 2003 Scaling relations for implantation of size-selected Au, Ag, and Si clusters into graphite. *Phys. Rev. Lett.* **90**, 055 503.

Richards, F. M. 1977 Areas, volumes, packing and protein structure. *Annu. Rev. Biophys. Bioeng.* **6**, 151.

Richards, D. P., Stathakis, C., Polakowski, R., Ahmadzadeh, H. & Dovichi, N. J. 1999 Labeling effects on the isoelectric point of green fluorescent protein. *J. Chromatogr. A* **853**, 21.

Robinson, R. C., Grey, L. M., Staunton, D., Vankelekom, H., Vernallis, A. B., Moreau, J. F., Stuart, D. I., Heath, J. K. & Jones, E. Y. 1994 The crystal-structure and biological function of leukemia inhibitory factor—implications for receptor-binding. *Cell* **77**, 1101.

Rossell, J. P., Allen, S., Davies, M. C., Roberts, C. J., Tendler, S. J. B. & Williams, P. M. 2003 Electrostatic interactions observed when imaging proteins with the atomic force microscope. *Ultramicroscopy* **96**, 37.

Sarno, D. M., Murphy, A. V., DiVirgilio, E. S., Jones, W. E. & Ben, R. N. 2003 Direct observation of

antifreeze glycoprotein-fraction 8 on hydrophobic and hydrophilic interfaces using atomic force microscopy. *Langmuir* **19**, 4740.

Schnyder, B., Kotz, R., Alliata, D. & Facci, P. 2002 Comparison of the self-chemisorption of azurin on gold and on functionalized oxide surfaces. *Surf. Interface Anal.* **34**, 40.

Tsodikov, O. V., Record, M. T. & Sergeev, Y. V. 2002 Novel computer program for fast exact calculation of accessible and molecular surface areas and average surface curvature. *J. Comput. Chem.* **23**, 600.

von Issendorff, B. & Palmer, R. E. 1999 A new high transmission infinite range mass selector for cluster and nanoparticle beams. *Rev. Sci. Instrum.* **70**, 4497.

Willner, I. & Willner, B. 2001 Biomaterials integrated with electronic elements: en route to bioelectronics. *Trends Biotechnol.* **19**, 222.

Zimmer, M. 2002 Green fluorescent protein (GFP): Applications, structure, and related photophysical behavior. *Chem. Rev.* **102**, 759.